**The EMBO Journal (2009) 28,** 3040–3051 | © 2009 European Molecular Biology Organization | All Rights Reserved 0261-4189/09
www.embojournal.org

THE EMBO JOURNAL

# Structural determinants for interaction of partial agonists with acetylcholine binding protein and neuronal α7 nicotinic acetylcholine receptor

**Ryan E Hibbs[1,5,7], Gerlind Sulzenbacher[2,7], Jianxin Shi[1,6], Todd T Talley[1], Sandrine Conrod[3], William R Kem[4], Palmer Taylor[1,*], Pascale Marchot[3] and Yves Bourne[2,*]**

[1]Department of Pharmacology, Skaggs School of Pharmacy and Pharmaceutical Sciences, University of California, San Diego, La Jolla, CA, USA, [2]Architecture et Fonction des Macromolécules Biologiques (AFMB, UMR-6098) CNRS, Université d'Aix-Marseille, Campus Luminy, Marseille, France, [3]ToxCiM, Département de Signalisation Neuronale, Centre de Recherche en Neurobiologie-Neurophysiologie de Marseille (CRN2M, CNRS UMR-6231), Université d'Aix-Marseille, Faculté de Médecine Secteur Nord, Marseille, France and [4]Department of Pharmacology and Therapeutics, College of Medicine, University of Florida, Gainesville, FL, USA

**The pentameric acetylcholine-binding protein (AChBP) is a soluble surrogate of the ligand binding domain of nicotinic acetylcholine receptors. Agonists bind within a nest of aromatic side chains contributed by loops C and F on opposing faces of each subunit interface. Crystal structures of *Aplysia* AChBP bound with the agonist anabaseine, two partial agonists selectively activating the α7 receptor, 3-(2,4-dimethoxybenzylidene)-anabaseine and its 4-hydroxy metabolite, and an indole-containing partial agonist, tropisetron, were solved at 2.7–1.75 Å resolution. All structures identify the Trp 147 carbonyl oxygen as the hydrogen bond acceptor for the agonist-protonated nitrogen. In the partial agonist complexes, the benzylidene and indole substituent positions, dictated by tight interactions with loop F, preclude loop C from adopting the closed conformation seen for full agonists. Fluctuation in loop C position and duality in ligand binding orientations suggest molecular bases for partial agonism at full-length receptors. This study, while pointing to loop F as a major determinant of receptor subtype selectivity, also identifies a new template region for designing α7-selective partial agonists to treat cognitive deficits in mental and neurodegenerative disorders.**

*The EMBO Journal* (2009) **28,** 3040–3051. doi:10.1038/emboj.2009.227; Published online 20 August 2009

*Corresponding authors. Y Bourne, Architecture et Fonction des Macromolécules Biologiques, UMR-6098, Case 932 - Campus de Luminy-163 Avenue de Luminy, F-13288 Marseille Cedex 09. Tel.: +33 4 91 82 55 66; Fax: +33 4 91 26 67 20; E-mail: yves.bourne@afmb.univ-mrs.fr or P Taylor, Department of Pharmacology, Skaggs School of Pharmacy and Pharmaceutical Sciences, University of California, San Diego, La Jolla, CA 92093-0657, USA. Tel.: +1 858 534 1366; Fax: +1 858 534 8248; E-mail: pwtaylor@ucsd.edu
[5]Present address: Vollum Institute, Oregon Health and Science University, Portland, OR, USA
[6]Present address: Genomics Institute of the Novartis Research Foundation, La Jolla, CA, USA
[7]These authors contributed equally to this work

**Received: 7 April 2009; accepted: 14 July 2009; published online: 20 August 2009**

*Subject Categories*: signal transduction; structural biology
*Keywords*: acetylcholine binding protein; anabaseine; crystal structure; nicotinic acetylcholine receptor; partial agonist

## Introduction

Nicotinic acetylcholine receptors (nAChRs) are prototypical cation-selective, ligand-gated ion channels (LGIC) that mediate fast neurotransmission in the central and peripheral nervous systems (Changeux and Edelstein, 2005; Taylor, 2006). The nAChRs belong to the Cys-loop superfamily of LGICs, that in mammals also includes the serotonin, $5HT_3$; γ-aminobutyric acids, GABA-A and GABA-C; and glycine receptors, and are formed by distinctive combinations of five subunits that confer selectivity in pharmacological properties and cellular location. The diversity of nAChR subunit assembly and subtype is most evident in the central nervous system, in which nine α and three β subunits have been defined.

The discovery of the acetylcholine binding protein (AChBP) from a freshwater snail, followed by its crystallographic analysis, showed a homopentameric assembly of subunits homologous to the N-terminal, extracellular ligand-binding domain (LBD) of the nAChR (Brejc *et al*, 2001). In addition to the overall primary and tertiary structural similarity of the subunits, the aromatic residues that form the ligand binding pocket at the subunit interface are highly conserved in the nAChR family, although the interface residues that contribute to the complementary face (or (−) face) show greater variability than those on the principal face (or (+) face). The binding pocket of AChBP possesses all the functional residues identified in the nAChR LBD, and extended areas of the subunit interface in the apical and membrane directions provide multiple means for selective accommodation of the many nicotinic ligands (Hansen *et al*, 2005). AChBP from *Aplysia californica* (A-AChBP), compared with its relatives from *Lymnaea stagnalis* (L-AChBP) and *Bulinus truncatus*, shows binding affinities and specificities similar to those of the neuronal, α7 nAChR subtype for nicotinic agonists and antagonists, as exemplified by its lower affinity for acetylcholine, but higher affinity for the α7-specific antagonistic α-conotoxin peptides (Hansen *et al*, 2002, 2004; Celie *et al*, 2004).

The coupling of AChBP with the pore domain of the $5HT_{3A}$ receptor not only results in acetylcholine binding with modest or intermediate affinity, characteristic of activatable receptors, but also triggers a low frequency opening of the ion channel (Bouzat *et al*, 2004), arguing for AChBP to be both a structural and functional surrogate for the extracellular LBD of nAChRs. A refined electron microscopy structure of the heteropentameric muscle-type, $\alpha 1_2\beta\gamma\delta$ nAChR, solved in part

 

using the AChBP template (Unwin, 2005), and the crystal structure of the extracellular domain of the isolated muscle-type α1 subunit bound to the peptide antagonist, α-bungarotoxin (Dellisanti *et al*, 2007), confirms the close structural similarity between the AChBP and nAChR subunits. A recent characterization of pentameric, prokaryotic LGICs shows their structural homology to AChBP and documents the similarity of their intra-subunit and inter-subunit arrangements (Bocquet *et al*, 2007, 2009; Hilf and Dutzler, 2008, 2009).

To date, AChBP offers the best template for obtaining high-resolution structures of the LBD of nAChRs. In turn, structural studies of AChBP in complex with a large variety of nAChR agonists and competitive antagonists have shown that loop C, found at the outer perimeter of the pentamer, adopts distinctive conformations upon agonist and antagonist occupation of the binding pocket (Bourne *et al*, 2005; Hansen *et al*, 2005), a phenomenon that can also be monitored in solution by hydrogen–deuterium exchange mass spectrometry (Shi *et al*, 2006). Overall, a 'core agonist signature motif' that recognizes the activating ligands was localized central to the binding pocket. In contrast to the small agonist molecules, the larger antagonists occupy an expanded surface area at the subunit interface resulting in further opening of loop C and often conferring a greater selectivity than the agonists do for receptor subtypes.

In comparison with full agonists or antagonists, partial agonists elicit only a fractional pharmacological response, even at full binding site occupation (Stephenson, 1956; Pratt and Taylor, 1990; Hoyer and Boddeke, 1993). Using state functions to describe receptor activation, partial agonism can be explained by the occupied ligand not shifting the conformational equilibrium between open and closed states fully to the open channel state (Pratt and Taylor, 1990). A recent proposal suggests that partial agonism in the nAChR superfamily is associated with a pre-open conformation that has a higher affinity for agonists than the resting receptor (Lape *et al*, 2008). In contrast to full agonists, partial agonists would have a diminished capacity to occupy the pre-open state before opening the channel. Irrespective of the mechanism and the structural description of the ligand-bound states, a ceiling on agonist efficacy can serve to minimize the toxicity upon overdose and reduce addiction liability of drugs. Achieving receptor subtype selectivity, affinities approaching or exceeding that of nicotine, and partial agonist characteristics for nAChR stimulation are all desirable features sought to improve nicotinic receptor-targeted therapies for neurodegenerative and psychiatric disorders (Kem, 2000; Hogg and Bertrand, 2007).

Recent studies have focused on a series of anabaseine-derived compounds showing a mixed pharmacological profile towards nAChRs (Briggs *et al*, 1995; de Fiebre *et al*, 1995; Kem *et al*, 1997, 2004). The parent molecule, anabaseine (Figure 1), is a natural nicotine-related pyridine alkaloid used by certain marine worms (Phylum *Nemertinea*, ribbon worms) as a chemical defense against predators and as a means for capturing prey (Kem *et al*, 2006a). It is a relatively non-selective nAChR agonist, but activates the muscle-type $\alpha 1_2\beta\gamma$(or ε)δ and neuronal α7 subtypes of nAChR with high potency and full efficacy (Kem *et al*, 1997). However, addition of a benzylidene group at the 3-position of the anabaseine tetrahydropyridine ring,

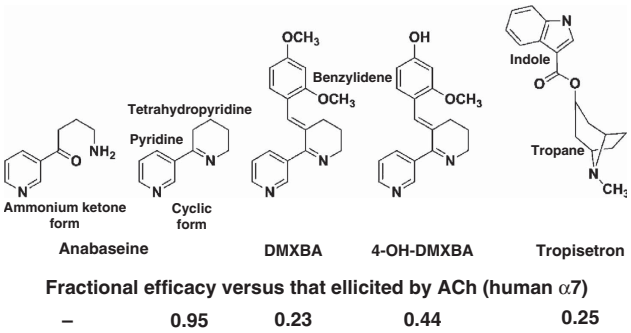


**Figure 1** Chemical structures and agonist efficacies towards human α7 nAChR of the ligands used in this study. The efficacy is the fractional response elicited by the agonist compared with the maximal response elicited by ACh. Values from: anabaseine: Stokes *et al* (2004); DMXBA and 4-OH-DMXBA: Kem *et al* (2004); Tropisetron: Papke *et al* (2005).

generating a benzylidene-substituted anabaseine (BA), is sufficient to confer functional selectivity for α7 nAChRs (de Fiebre *et al*, 1995; Papke *et al*, 2004). The large number of BA analogues synthesized using various substituents on the benzylidene ring and varying degrees of agonist efficacy provide a series of congeners well suited for a detailed analysis of ligand binding sites of nAChRs and AChBPs. Moreover, the BA analogues show unique absorption and fluorescence emission properties that enable one to describe the protonation state of the bound ligand, and the permittivity and polarizability of the surrounding side chains in the binding site (Talley *et al*, 2006).

The BA derivative, 3-(2,4-dimethoxybenzylidene)-anabaseine (DMXBA, Figure 1) is also a promising drug candidate, as the added hydrophobic substituents favour the penetration of the blood–brain barrier and confer partial agonist activity at the α7 receptor. DMXBA is in clinical trials for cognition enhancement and improvement of auditory gating in schizophrenia (Olincy *et al*, 2006; Freedman *et al*, 2008). It also shows neuroprotective properties (Martin *et al*, 1994; Shimohama *et al*, 1998). After oral administration, DMXBA is transformed into three hydroxy metabolites, 2-OH-, 4-OH- and 2,4-di-OH-DMXBA, which show binding affinities and partial agonist properties superior to the parent compound found on rat and human α7 nAChRs (Kem *et al*, 2004). However, these metabolites are more polar than DMXBA and cross the blood–brain barrier less readily, potentially limiting their use as therapeutic agents targeting the central nervous system. DMXBA and its hydroxy metabolites are low potency antagonists at the human $5HT_3$ receptor; the metabolites are partial agonists at the murine $5HT_3$ receptor (Machu *et al*, 2001; Zhang *et al*, 2006).

Tropisetron was initially developed as a high affinity antagonist for $5HT_3$ receptors. More recently, it was identified as a partial agonist selective for the α7 receptor and an antagonist for non-α7 receptors (Macor *et al*, 2001). In several countries, it is used to alleviate chemotherapy-induced nausea and vomiting (Ho and Gan, 2006). Tropisetron contains bicyclic tropane and hydrophobic indole moieties, in which the bridged aza-nitrogen and indole ester components may adopt similar positions, respectively, to the imine-nitrogen and pyridine ring components of the anabaseines (Figure 1). Moreover, various tropine esters

show pharmacological activities similar to the BA α7-selective partial agonists.

To understand the structural determinants that confer partial agonist character and dictate nAChR subtype selectivity, we have carried out a comprehensive structural study of α7-selective partial agonists using A-AChBP as a surrogate of the extracellular LBD of the α7 nAChR. The crystal structures of A-AChBP bound with the non-selective full agonist anabaseine, two α7-selective benzylidene-anabaseine derivatives, DMXBA and 4-OH-DMXBA, and the α7-selective, though chemically-distinct, tropisetron, were solved to 2.7–1.75 Å resolution range. These structures show at least two modes of binding of partial agonists and identify essential interactions contributing to the high affinity binding of these compounds to the α7 nAChR.

## Results and discussion

### *Overall views of the structures*

The structures of the A-AChBP complexes with anabaseine, the BA derivatives DMXBA and 4-OH-DMXBA, and tropisetron (Figure 1), were solved from crystals grown in three distinct space groups associated with different packing geometries, with virtually no contribution of the tip of loop C towards crystal packing contacts (see, Materials and methods; Table I). All structures show the tight homopentameric ring assembly of subunits found in previous AChBP structures (Figure 2).

Out of several loops that emerge from the β-sandwich core of each subunit, five (loops β3–β4 (or A), β7–β8 (or B), β9–β10 (or C), β8–β9 (or F), and the conserved Cys-loop) have been shown to be critical for nAChR function, with several of their residues being involved in both subunit assembly and ligand binding (Malany *et al*, 2000; Karlin, 2002). The ligand binding pocket corresponds to a nest of five electron-rich aromatic side chains provided by Tyr 93, Trp 147, Tyr 188, Tyr 195 on the (+) face and Tyr 55 on the (−) face of the interface. The binding pocket is partially sheltered from the outside solvent by loop C, which harbours a disulfide bridge linking the vicinal Cys 189 and Cys 190 residues at its tip, a signature motif for nAChR α-subunits.

Apart from the anabaseine complex (see, Materials and methods), the structures show well-defined electron densities indicative of high occupancy of all five subunit interfaces by the bound ligands (Figure 2). The structures, and their comparison with earlier structures of AChBP, free of a bound nicotinic ligand (Hansen *et al*, 2005), and in complex with the full-agonists, nicotine (Celie *et al*, 2004) and epibatidine (Hansen *et al*, 2005), define the structural determinants at the subunit interfaces and conformational adaptations associated with the binding of distinct partial agonists selective for nAChR subtypes.

**Table I** Data collection and refinement statistics

| | Anabaseine | DMXBA | 4-OH-DMXBA | Tropisetron |
|---|---|---|---|---|
| *Data collection* | | | | |
| Beam line | ID23-EH2 | ID23-EH1 | ALS-8.2.2 | ID23-EH1 |
| Space group | C2 | $P2_12_12_1$ | $P2_12_12_1$ | I23 |
| Cell dimensions | 84.25, 125.77, 257.0 | 87.22, 114.80, 131.28 | 86.91, 115.39, 130.61 | 212.58, 212.58, 212.58 |
| *a*, *b*, *c* (Å), β (deg) | 95.4 | | | |
| Resolution (Å)[a] | 70–2.7 (2.85–2.7) | 47–1.80 (1.94–1.80) | 57–1.75 (1.84–1.75) | 87–2.20 (2.32–2.20) |
| $R_{merge}$ (%)[b] | 7.3 (47.2) | 6.4 (49.5) | 5.1 (38.6) | 8.8 (49.7) |
| $\langle I/\sigma I \rangle$ | 25.1 (4.2) | 16.8 (2.4) | 20.7 (4.5) | 13.9 (3.4) |
| Completeness (%) | 99.9 (99.8) | 99.9 (99.9) | 99.7 (99.5) | 100 (100) |
| Redundancy | 6.5 (6.5) | 4.3 (4.3) | 3.3 (3.2) | 5.8 (5.9) |
| B from Wilson plot (Å$^2$) | 37.8 | 23.6 | 24.1 | 35.7 |
| *Refinement* | | | | |
| Resolution (Å) | 2.7 | 1.80 | 1.75 | 2.20 |
| Number of reflections | 70727 | 116030 | 125779 | 78146 |
| $R_{work}/R_{free}$[c] | 20.18/25.06 | 16.85/20.6 | 16.96/20.31 | 17.73/21.17 |
| Number of atoms | 17351 | 9657 | 9371 | 9207 |
| Protein | 16874 | 8486 | 8406 | 8491 |
| Ligand/sugar/other | 112/42/16 | 115/64/— | 110/75/0 | 105/0/0 |
| Water | 307 | 992 | 780 | 611 |
| *B-factors (A$^2$)* | | | | |
| Protein Main/side chain | 39.7/41.3 | 33.1/35.8 | 29.6/33.8 | 35.6/37.9 |
| Ligand/sugar/others | 40.3/37.5/65.3 | 34.9/60.2/ | 33.3/52.7/— | 32.6/—/— |
| Water | 35.3 | 39.9 | 38.1 | 36.8 |
| *r.m.s.d. values*[d] | | | | |
| Bond lengths (Å) | 0.007 | 0.015 | 0.014 | 0.013 |
| Bond angles (deg) | 1.10 | 1.507 | 1.489 | 1.464 |
| PDB accession code | 2WNL | 2WNJ | 2WN9 | 2WNC |

[a]Values in parentheses are those for the last shell.
[b]$R_{merge} = \Sigma_{hkl} \Sigma_i |I_{i(hkl)} - \langle I_{hkl} \rangle| / \Sigma_{hkl} \Sigma_i I_{i(hkl)}$, where $I$ is an individual reflection measurement and $\langle I \rangle$ is the mean intensity for symmetry-related reflections.
[c]$R_{cryst} = \Sigma_{hkl} ||Fo| - |Fc|| / \Sigma_{hkl} |Fo|$, where Fo and Fc are observed and calculated structure factors, respectively. $R_{free}$ is calculated for 3% of randomly selected reflections excluded from refinement, except for DMXBA transferred from the 4-OH-DMXBA dataset.
[d]r.m.s.d. from ideal values.

 

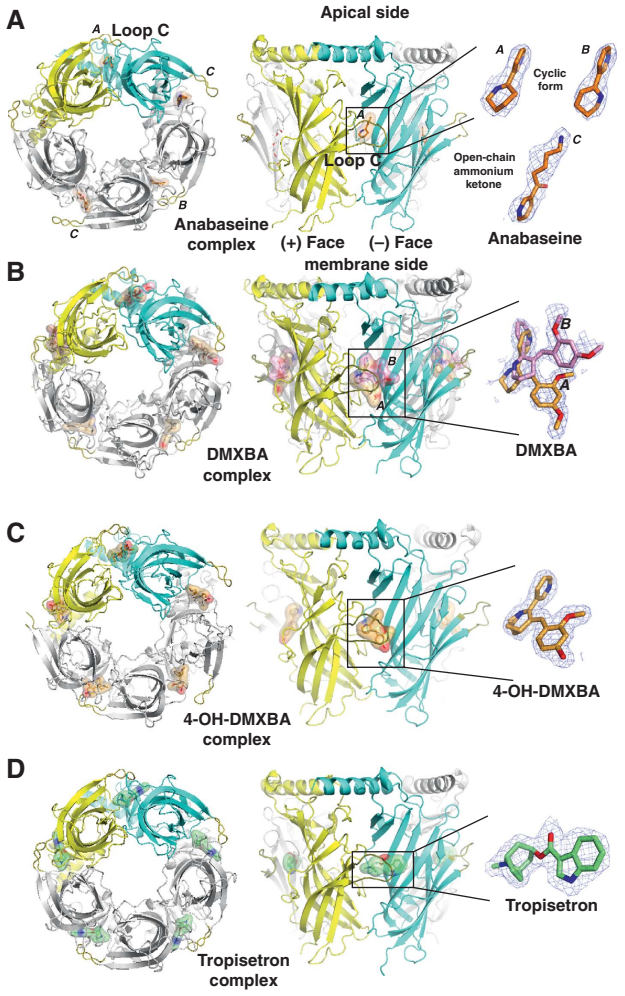


**Figure 2** The four pentameric full and partial agonist–AChBP complexes: overall views. (**A**) Anabaseine (orange bonds), (**B**) DMXBA (bright orange and pink), (**C**) 4-OH-DMXBA (light orange) and (**D**) tropisetron (green) are shown as bound at each subunit interface. In the first column, the four A-AChBP pentamers are viewed from their 'membrane' side. The conformational flexibility of the tip of the loop C is clearly visible. In the second column, the pentamers are oriented with their apical N-terminus at top and their 'membrane' side C-terminus at bottom. The bound ligands are shown through a transparent surface. Third column shows close-up views of the bound ligands with their 2.7–1.75 Å resolution 2Fo–Fc electron density maps contoured at 1.0 σ (blue). The subunits contributing the (+) and (−) faces of one interface are shown in yellow and cyan, respectively. The ligands are shown with red oxygen and blue nitrogen atoms.

### *The anabaseine complex*

Anabaseine is a full agonist at muscle-type and α7 nAChRs (Figure 1; Table II). Similar to nicotine and its analogues, anabaseine is composed of a non-aromatic tetrahydropyridine ring attached to the 3-position of an aromatic pyridine ring. However, in the anabaseine tetrahydropyridine ring, the imine double bond is electronically conjugated to the aromatic ring, instead of being an isolated tertiary or secondary amine as in nicotine or epibatidine.

In two out of the five binding sites in the pentamer, the cyclic form of anabaseine adopts two distinct conformations, A and B, that differ by a 90° rotation of the tetrahydropyridine ring relative to the pyridine ring (Figure 2A). Instead of retaining the predicted co-planar conformation (Supplementary Table I), the two rings (tetrahydropyridine and pyridine) are twisted by ∼35° and ∼45° relative to each other, as found for the bound nicotine (Celie *et al*, 2004). In conformer A, the imine nitrogen is properly positioned to form a hydrogen bond (∼2.7 Å) with the carbonyl of Trp 147 on the (+) face of the interface (Figure 3). The tetrahydropyridine ring in anabaseine is bound in a position similar to the pyrrolidine ring in nicotine (Celie *et al*, 2004) and the bridged nitrogen in epibatidine (Hansen *et al*, 2005). The tetrahydropyridine ring in anabaseine which, compared with the pyrrolidine ring of nicotine, is larger and tilted by ∼80° towards loop C, adopts a flattened boat conformation. The ring establishes near face-to-edge stacking interactions with Trp 147 on the (+) face and Tyr 188 in loop C, and face-to-face interactions with Tyr 195 at the hinge point of loop C and the Cys 190–Cys 191 disulfide at its tip. In conformer B, the rotated tetrahydropyridine ring loses its hydrogen bond with Trp 147 but maintains an optimal interaction with the nest of aromatic residues. The pyridine nitrogen is hydrogen bonded, through a bridging water molecule, to the main chains of residues Ile 106 and Ile 118, as previously observed for nicotine (Celie *et al*, 2004) and the neonicotinoids: imidacloprid and thiacloprid (Talley *et al*, 2008). Residues Val 108, Met 116, Ile 118 and Val 148 also form van der Waals contacts with the anabaseine pyridine ring. In contrast to its contribution in the nicotine and epibatidine complexes, Tyr 93 at the base of the binding pocket is shifted away (by ∼1.5 Å) from anabaseine and only weakly contributes to its binding (Figure 3).

The mode of binding of the cyclic form of anabaseine, wherein aromatic residues from loop C contribute to stabilization of the tetrahydropyridine ring, is similar to those of the other full agonists, nicotine and epibatidine (Figure 3). In turn, loop C adopts a conformation similar to that seen in complexes with full agonists with the disulfide that abuts at the midpoint between the two rings (Celie *et al*, 2004; Hansen *et al*, 2005). In the tetrahydropyridine ring of anabaseine, the absence of a protruding *N*-methyl group pointing toward loop C, as found in nicotine or the nitrogen-containing alicyclic skeleton (bridge ring) in epibatidine, could be responsible for the lower affinity of anabaseine for A-AChBP (Table II). The lack of tight interaction between anabaseine and Tyr 55 on the (−) face may contribute to the relatively low affinity of anabaseine for A-AChBP. In L-AChBP and rat brain α7, the bulky Trp side chain that replaces A-AChBP Tyr 55 on the (−) face most probably contributes to the respective 4-fold and 17-fold higher affinity (Table II), consistent with additional stacking interactions with the anabaseine tetrahydropyridine ring (Figure 3).

In the third binding site, the open chain ammonium ketone of anabaseine is present with an open conformation of loop C, whereas in the fourth binding site, the closed form overlaps with the open chain form associated with a non-tethered loop C (Figure 2A). The mode of binding of the open form of anabaseine (conformer C) largely differs from that of the closed form by a flip of the molecule such that the pyridine ring is shifted 7 Å outward and the ammonium group lies within the binding pocket. In one binding site, the open chain form is bound in the opposite direction, with the pyridine ring in stacking interaction with Trp 147, whereas the ammonium group points toward the solvent. Only the cyclic form

**Table II** Ligand dissociation constants for A- and L-AChBP and other Cys loop receptors

| Ligand | A-AChBP ($K_d$, nM) | L-AChBP ($K_d$, nM) | Rat α7 ($K_d$, nM) | Rat α4β2 ($K_d$, nM) | Rat 5HT3 ($K_d$, nM) | Human 5HT3 (IC50, μM) |
|---|---|---|---|---|---|---|
| Anabaseine | >1000[a] | 240 ± 21[a] | 200 ± 24[b] | 110 ± 14[b] | — | — |
| DMXBA | 330 ± 58[a] | 19 ± 1[a] | 130 ± 14[c] | 253 ± 37[c] | — | 3.1[d] |
| 4-OH-DMXBA | 3.0 ± 0.96[a] | 0.43 ± 0.03[a] | 235 ± 14[c] | 69 ± 30[c] | — | 7.4[d] |
| 2-OH-DMXBA | 220 ± 26[a] | 12 ± 3[a] | 317 ± 67[c] | 387 ± 25[c] | — | 1.5[d] |
| Tropisetron | 479 ± 57[e] | 74 ± 6[e] | 6.9 ± 2.4[f] | 55 000 ± 28 000[f] | 5.3 ± 3.0[f] | — |

[a]Talley *et al*, 2006 (AChBP $K_d$ values were measured by the displacement of the agonist [$^3$H] epibatidine).
[b]Kem *et al*, 1997 (α7 $K_d$ value measured by the displacement of the antagonist $^{125}$I-α-bungarotoxin; α4β2 $K_d$ value measured by the displacement of the partial agonist [$^3$H]-cytisine).
[c]Kem *et al*, 2004 (α7 $K_d$ value measured by the displacement of the antagonist $^{125}$I-α-bungarotoxin; α4β2 $K_d$ value measured by the displacement of the partial agonist [$^3$H]-cytisine).
[d]Zhang *et al*, 2006 (IC50 represents median inhibitory concentration for antagonism of 5HT evoked currents with human 5HT3A receptors expressed in *Xenopus* oocytes).
[e]This study (AChBP $K_d$ values measured by displacement of the agonist [$^3$H] epibatidine).
[f]Macor *et al*, 2001 (α4β2 $K_d$ value measured by displacement of the partial agonist [$^3$H]-cytisine).

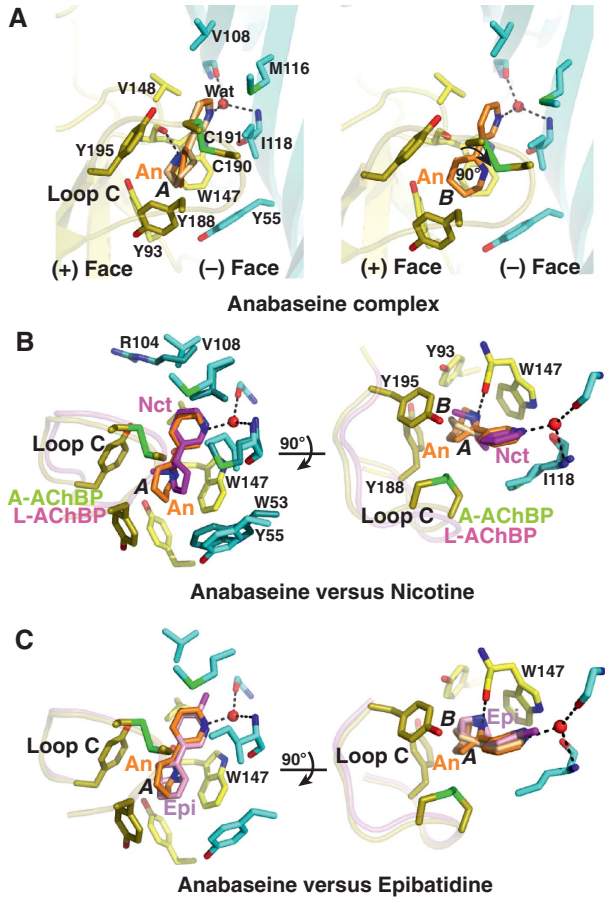


**Figure 3** The anabaseine–AChBP complex: close-up view and structural comparisons. (**A**) The subunit interface is oriented with its apical side at top and its 'membrane' side at bottom (same orientation as in Figure 2, column 2). The tip of loop C harbouring the Cys 190–Cys 191 disulfide is highlighted in green. The high affinity cyclic form of anabaseine, conformer A (left) and B (right), is bound between the disulfide above it and Trp 147 below it. Side chains and solvent molecules that interact specifically with bound anabaseine are shown. Critical hydrogen bond with the Trp 147 carbonyl is observed in conformer A. Superimposition of anabaseine bound to A-AChBP (conformers A and B) with (**B**) nicotine bound to L-AChBP (Celie *et al*, 2004) and (**C**) epibatidine bound to A-AChBP (Hansen *et al*, 2005), viewed in two orientations rotated by 90°. Retention of the closed conformation of loop C is evident.

binds with significant affinity to the ACh binding site of muscle and neuronal nAChRs (Kem *et al*, 2006b). The lack of full site occupancy of the pentameric AChBP by anabaseine relates to the presence of comparable amounts of the cyclic and ring opened ammonium ketone forms at the pH used for crystallization.

### *The DMXBA complex*

The structure of A-AChBP in complex with DMXBA shows an agonist molecule tightly associated with each of the five subunit interfaces (Figures 1 and 2B). As in the anabaseine complex, a similar network of hydrogen bonds is involved in ligand binding, with the protonated imine nitrogen ideally positioned to target the Trp 147 carbonyl oxygen, ~2.75 Å away, whereas the pyridine amine is bound to Ile 106 and Ile 118 main chains through a water molecule (Figure 4). As expected from the bathochromic shifts in the bound DMXBA–AChBP complex (Talley *et al*, 2006), aromatic interactions are also conserved with near parallel stacking of the pyridine ring with the Trp 147 indole ring, whereas the tetrahydropyridine ring makes close contact with the Tyr 93 phenolic ring on the membrane side of the (−) face. The benzylidene ring, which confers α7 selectivity, protrudes from the binding pocket in a direction parallel to the radial axis of the AChBP pentamer. The benzylidene ring readily extends the network of interactions beyond the anabaseine core by interacting with residues from the (+) and (−) faces outside the binding pocket. In comparison with its position in the anabaseine complex, in the DMXBA complex the anabaseine core is slightly displaced (by 0.5 Å) and tilted (by ~15°) towards the 'membrane' side of the binding pocket.

In three out of the five binding sites in the pentamer, DMXBA adopts two alternate orientations, A and B, present in roughly equal populations (Figure 2B; Supplementary Table I). The two DMXBA orientations differ by a translational (1.5 Å) and rotational (~25°) drift motion of the anabaseine core which is associated with a ~50° arc motion of the benzylidene ring, resulting in a ~90° arc motion of the Tyr 55 phenol ring and a ~50° rotation of the Tyr 93 side chain (Figure 4). In comparison with the anabaseine complex, the two alternative orientations of the anabaseine core in DMXBA are positioned on both sides of the position occupied by anabaseine. In turn, a slightly weaker hydrogen

 

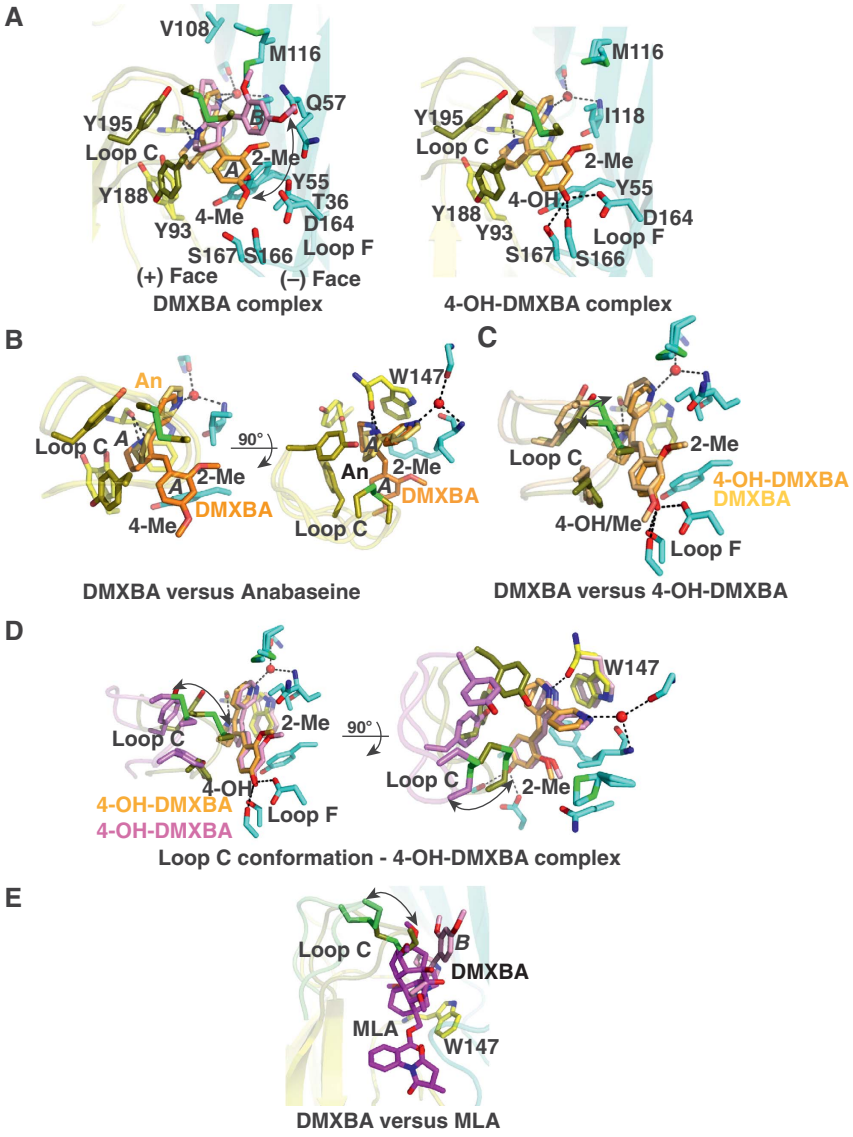


**Figure 4** The DMXBA–AChBP and 4-OH-DMXBA–AChBP complexes: close-up view and structural comparisons. (**A**) DMXBA (left) and 4-OH-DMXBA (right) bound to A-AChBP (same orientation as in Figure 2, column 2). DMXBA orientations A and B are indicated. (**B**) Superimposition of DMXBA bound to A-AChBP (orientation A) with anabaseine bound to A-AChBP (conformer A), viewed in two orientations rotated by 90°. (**C**) Superimposition of DMXBA (orientation A) bound to A-AChBP with 4-OH-DMXBA bound to A-AChBP, oriented as in panel A. (**D**) Superimposition of two 4-OH-DMXBA molecules bound at two distinct subunits interfaces, viewed in two orientations rotated by 90°. (**E**) Superimposition of DMXBA bound to A-AChBP (orientation B) with MLA bound to A-AChBP.

bond (3.0 versus 2.7 Å) is predicted between the imine nitrogen and Trp 147 carbonyl in orientation B of the bound DMXBA compared with orientation A. In orientation A, the benzylidene ring is sandwiched between Tyr 188 in loop C on the (+) face and Tyr 55 on the (−) face and projects the distal 4-methoxy group towards a polar side chain triad of Asp 164, Ser 166 and Ser 167 in loop F and close to Thr 36 (3.5 Å) in strand β1 on the (−) face (Figure 4). The 2-methoxy group points in an apical direction to interact with Thr 36, Gln 57 and Ile 118. In orientation B, the rotated benzylidene ring abuts against Cys 190 and is sandwiched between the tip of loop C on the (+) face and Ile 118 on the (−) face. In turn, the 4-methoxy and 2-methoxy groups point towards the solvent and weakly interact with the side chains of Met 116 and Gln 57, respectively. The benzylidene ring of DMXBA points in a direction roughly parallel to the axis of the bulky lycoctonine skeleton of the antagonist methyllycaconitine (MLA) (Figure 4E). In the other two binding sites in the pentamer, the benzylidene ring adopts orientation A favouring interaction with loop F.

Although DMXBA adopts two distinct positional orientations within the binding pocket, the same loop C position is retained (Figures 2B and 4). In fact, the solvent-exposed benzylidene ring in the two orientations prevents loop C from adopting the closed conformation seen for the smaller full agonists, nicotine, epibatidine and anabaseine. Instead, the loop C conformational position is an intermediate between those observed for the full agonists and for ligand-free A-AChBP, respectively (Celie *et al*, 2004; Hansen *et al*, 2005).

### *The 4-OH-DMXBA complex*

The structure of A-AChBP in complex with the 4-hydroxy metabolite of DMXBA, 4-OH-DMXBA (Figures 1 and 2C), shows a ligand molecule tightly bound at each subunit

interface, with a position and orientation similar to those seen for conformation A of DMXBA (Supplementary Table I). In turn, a similar network of hydrogen bonds and aromatic interactions is observed for the anabaseine core and the benzylidene ring in the two complexes (Figure 4). However, in contrast to the DMXBA complex, loop C in the 4-OH-DMXBA complex adopts two distinct conformations. In two of the five binding sites, loop C tightly packs against a buried benzylidene ring, with Cys 190 making contact with the ring system, and it is displaced outwards by ~2.5 Å relative to its position in structures of AChBP bound to full agonists. In two other binding sites, the tip of loop C does not interact with the benzylidene ring but instead moves outward, by ~7 Å, to adopt an open conformation reminiscent of that seen in ligand free, anabaseine-bound and DMXBA-bound AChBPs. In the fifth binding site, the tip of loop C is sufficiently disordered to not be visible. Overall, the extent of the loop C opening-to-closure movement on 4-OH-DMXBA binding is up to ~5.5 Å, and this fluctuation is associated with a 0.5 Å outward/radial displacement of the entire 4-OH-DMXBA molecule (Figure 4). However, this movement barely affects (~0.2 Å) the hydrogen bond distance between the imine nitrogen and the Trp 147 carbonyl.

Binding experiments have established that 4-OH-DMXBA, with its nanomolar $K_d$ (Table II), shows the highest affinity among a set of related anabaseines for A-AChBP (Talley *et al*, 2006). Accordingly, the structural data highlight a more favourable polar environment of loop F to accommodate the 4-hydroxyl group of the benzylidene ring. Indeed, substitution of a methyl group to create the 4-methoxy group in DMXBA creates steric clashes between the methyl and the polar environment of loop F to generate a less favourable, alternate conformation B; consistent with a 110-fold decrease in affinity of DMXBA compared with the more potent 4-OH-DMXBA metabolite (Talley *et al*, 2006). In contrast, the presence of a hydroxyl or a methyl group at the 2-position only moderately affects binding affinity, consistent with greater solvent exposure at this position. In turn, we speculate that 2-OH-DMXBA, when bound, adopts a position similar to that of DMXBA. The importance of having a hydrogen bond-forming moiety at the 4-position is emphasized in the binding data wherein the four BA congeners with the highest affinity for A-AChBP have either a hydroxyl or an amino substitution at the 4-position of the benzylidene ring (Talley *et al*, 2006). Moreover, our difference spectroscopic analysis shows that in bound 4-OH-DMXBA, both the tetrahydropyridine nitrogen and the phenolic oxygen are protonated. The red shifted peak at 550 nm, characteristic of the zwitterion containing a cationic amine and phenolate anion as a dominant species in solution at pH 7.5, is not evident in the bound species (Talley *et al*, 2006).

### *The tropisetron complex*

The structure of A-AChBP in complex with tropisetron shows a tightly bound ligand in all five binding sites, with the main axis of the ligand nearly perpendicular to the pentameric five-fold symmetry axis (Figures 1 and 2D). The tropane-bridged ring, with its piperidine moiety in the chair conformation, is positioned similar to the smaller pyrrolidine ring of nicotine or the nitrogen-containing bicyclic skeleton of epibatidine bound to AChBP (Celie *et al*, 2004; Hansen *et al*, 2005) (Figure 5). However, the tertiary amine of the tropine

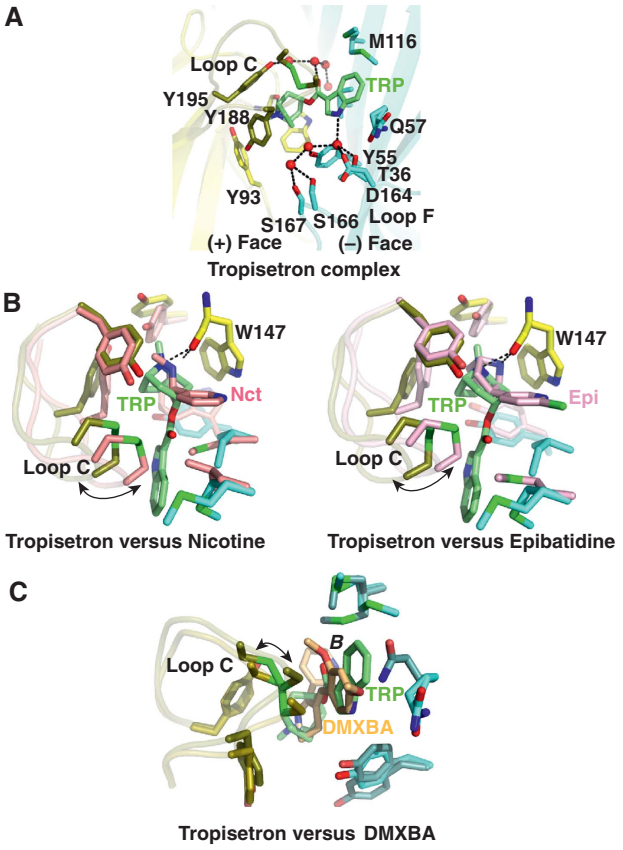


**Figure 5** The tropisetron–AChBP complex: close-up view and structural comparisons. (**A**) The A-AChBP subunit interface in the tropisetron complex (same orientation as in Figure 2, column 2). (**B**) Superimposition of tropisetron bound to A-AChBP with (left) nicotine bound to L-AChBP (Celie *et al*, 2004) and (right) epibatidine bound to A-AChBP (Hansen *et al*, 2005). (**C**) Superimposition of tropisetron and DMXBA (orientation B) bound to A-AChBP; their benzylidene and indole rings occupy similar positions at the subunit interface.

establishes a slightly longer hydrogen bonding distance (3.1 Å) from the Trp 147 carbonyl than seen for nicotine and epibatidine. The *N*-methyl group in the tropane ring is lodged between Tyr 93, Trp 147, Tyr 188, Tyr 195 from the (+) face and Tyr 55 from the (−) face within the aromatic nest. The 100-fold lower α7-selective agonist activity of the simple compound tropane (or tropinone) compared with tropisetron likely results from the positioning of the tropane ring by the methyl group and the contribution of the exocyclic indole ester (Papke *et al*, 2005). The carbonyl oxygen in the ester linkage between the indole and tropane moieties contributes to stabilize a network of four water molecules located in the apical portion of the interface. The tropisetron indole ring extends radially away from the binding pocket to point towards the complementary subunit. The indole ring is sandwiched between Ile 118 and the tip of loop C, with Cys 190 that abuts on the pyrrole ring. It also interacts with Tyr 55, Gln 57 and Met 116 on the (−) face. The side chains of the latter three residues are substantially shifted from their positions in the DMXBA and 4-OH-DMXBA complexes to accommodate the bulky indole ring of tropisetron. The indole nitrogen points towards loop F and interacts with Thr 36 and Asp 164 through a solvent molecule. The position of the

indole group relative to the (−) side of the binding pocket is similar to the position of the benzylidene ring in conformation B of bound DMXBA. Consequently, the position and closed conformation of loop C are similar in these two structures: in the tropisetron complex the tip of loop C is only slightly displaced outwards (∼1 Å) from its position in the DMXBA complex.

### *The pH dependence of ligand binding*

Several types of data indicate that the receptor-binding form of most nAChR ligands, including the anabaseines, is the cationic species. The previously reported absorption difference spectra for the BA derivatives show that the bound species is found in a region of low permittivity and high polarizability, reflecting the abundance of aromatic side chains surrounding the bound ligand (Talley *et al*, 2006). Moreover, the ionization profiles show the imine hydrogen to be protonated in anabaseine, DMXBA and 4-OH-DMXBA, establishing that the necessary proton is present to establish hydrogen bonding between the imine and the carbonyl oxygen of Trp 147 (Figure 6). Indeed, the imine nitrogen in the anabaseine core in the three compounds progressively loses its proton (and the affinity for the compound decreases) as pH increases from 6.0 to 9.0 (Kem *et al*, 2004; Talley *et al*, 2006). The benzylidene anabaseines do not show ring opening, due to π-electron resonance stabilization of the imine by the benzylidene moiety. However, in the case of 4-OH-DMXBA, an additional ionization state (deprotonation of the phenolic hydroxyl) is present. However, it seems from the shift in binding at pH 9.0 that the bound species retains the phenolic hydrogen rather than existing as a zwitterion with the iminium and phenolate. This further establishes the importance of hydrogen bonding through the donor phenol in the bound state of the complex. In contrast to the anabaseines, tropisetron does not show an appreciable pH dependence of binding over the range of 6.0–9.0 (Figure 6). Tropine esters are strong bases with pKa values between 9.8 and 10.0. As such, the bound form should be the protonated species, which is present in appreciable abundance between pH 6.0 and 9.0.

### *Partial versus full agonists*

Our study using non-selective and α7-selective agonists highlights several features that shed light on the behaviour of receptor/LBD conformations associated with the binding of partial agonists. First, our structural studies show that ligands with partial agonist characteristics adopt multiple conformations in the bound state (Figure 7). Second, a slight increase in the hydrogen bond distance between the secondary and tertiary amines (the iminium nitrogen is formally a strained tertiary amine) and the backbone carbonyl oxygen on Trp 147, a conserved residue on the (+) face of the binding site, is a conserved feature amongst these ligands. Finally, the loop C position associated with partial agonist binding is not only intermediate between the distinctive positions for agonists and antagonists but also varies between binding sites on the same homomeric pentamer (Figure 7). This again suggests that loop C undergoes rapid opening and closing events around a vacant binding site (Bourne *et al*, 2005; Shi *et al*, 2006). In turn, occupation by full versus partial agonists may result in different ligand orientations that are coupled to particular conformations of loop C. The DMXBA- and 4-OH-DMXBA-AChBP structures also indicate that a ligand serving as a partial agonist may adopt a binding pose or configuration at one site distinct from that of a second site within the same pentameric receptor. Indeed, one of the two orientations of

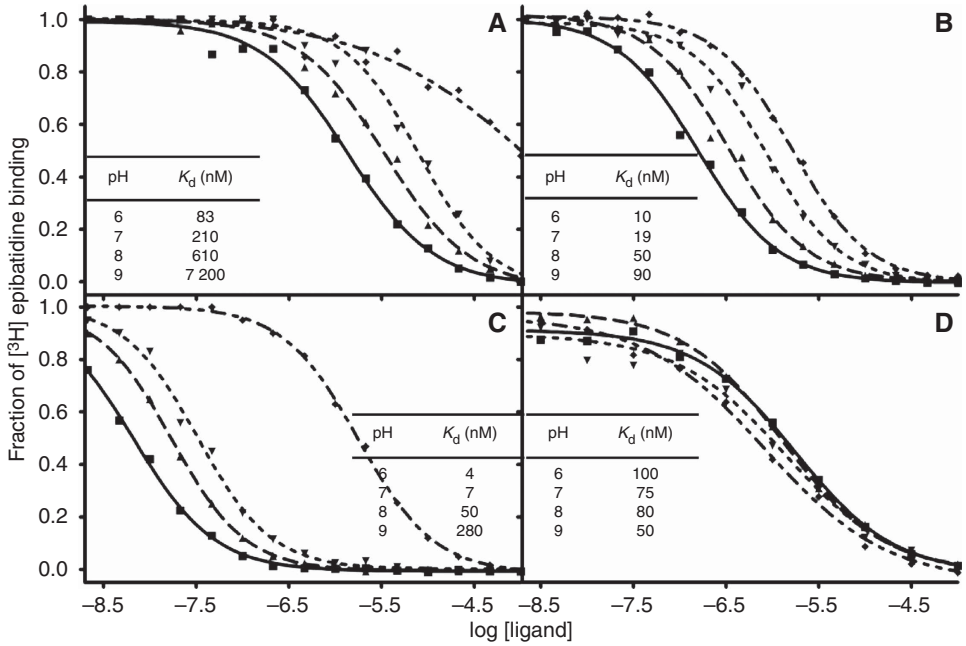


**Figure 6** The pH dependence of the binding of the four agonists to AChBP. Competition between the binding of (**A**) anabaseine, (**B**) DMXBA, (**C**) 4-OH-DMXBA and (**D**) tropisetron with that of [3H]–epibatidine (pKa = 10.1) to L-AChBP at various pH values, using 0.1 M phosphate/pyrophosphate buffered at pH 6 (■), 7 (▲), 8 (▼) and 9 (◆).The pH dependence of the binding of anabaseine, as well as of the two BAs (Talley *et al*, 2006), is consistent with the protonated imine (pKa = 7.6) being the bound species. In contrast, the absence of a detectable pH dependence for tropisetron binding in this pH range is consistent with the cationic character of the tropine ester (pKa = 9.8–10.0).

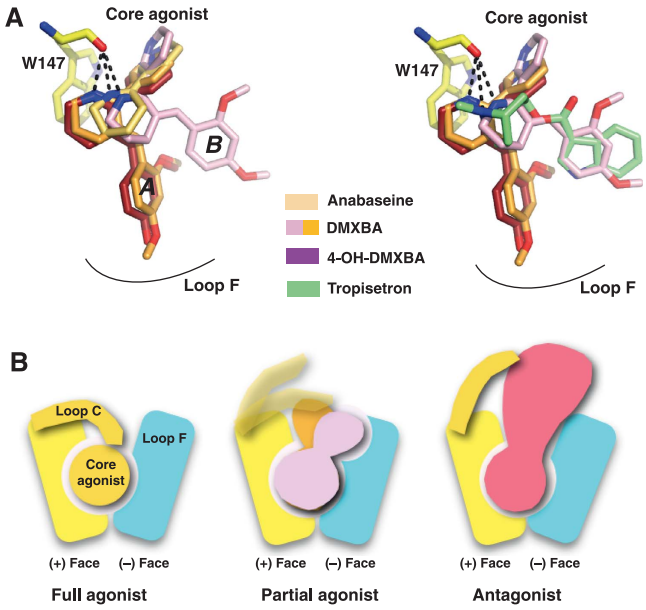


**Figure 7** Modes of binding of the nicotinic ligands. (**A**) Overlap view of the superimposed bound ligands. (**B**) Schematic representation of the binding modes of a nicotinic full agonist (left), partial agonist (centre) and antagonist (right) to AChBP. The (+) and (−) faces of one subunit interface are symbolized along with loop C, whose positional conformation varies on binding of the various nicotinic ligands.

the weak partial agonist DMXBA resembles that of the MLA antagonist, whereas the single orientation of the much more efficaceous 4-OH-DMXBA resembles that for agonists (such as lobeline). In other words, orientation A could be that of an agonist, whereas orientation B would be closer to that of an antagonist. A multiplicity of bound nAChR states for partial agonists provides another mechanism for achieving intermediate efficacies for partial agonists. Distinct conformations of congeneric competitive antagonists are found at the ligand binding pocket of AChBP (Gao *et al*, 2003). Our study is the first to show that partial agonists may also display multiple orientations within the five separate sites in a homomeric pentamer.

Although the soluble AChBP faithfully reflects the recognition properties of nAChRs for nicotinic ligands extending across the range of agonists and antagonists, it probably lacks the capacity to attain all of the conformational states of a functioning receptor tethered to an intrinsic membrane channel. The observation that AChBP fails to show cooperativity upon sequential occupation of its sites by agonist reflects the case in point (Hansen *et al*, 2002). Despite significant variations in chemical structure, the BAs and tropisetron contain substituted ring systems extending from a hydrogen bond donor of a protonated nitrogen in the imine or tropine. A second common feature of these partial agonists resides in the size of the substituents and their radial orientation when bound, extending their interaction surface outside the binding pocket to a region near loop F on the (−) face. In turn, the substituents control the degree of loop closure and prevent loop C from wrapping around the bound ligand as occurs for full agonists (Figure 7) (Celie *et al*, 2004; Hansen *et al*, 2005). Instead, loop C undergoes only limited opening and closure movements and adopts, throughout the five binding sites of a same pentamer, a range of positions as yet uniquely observed for this class of ligands. Recent findings, suggesting that partial and full agonists may interact differently with the binding site that undergoes conformational changes attendant on ligand binding (Lape *et al*, 2008), are consistent with our structural observations.

### *Ligand selectivity for nAChR subtypes*

Anabaseine presents a standard pharmacophore structure, similar to that of nicotine, allowing it to activate α7, muscle and other nAChR subtypes. The addition of the benzylidene group is responsible for the loss of agonist activity at subtypes other than α7. The activity profile of tropisetron is similar to those of the BA α7-selective partial agonists, such as DMXBA or 4-OH-DMXBA. Although tropane and some related agonists containing an additional nitrogen bridging ring (e.g. epibatidine and TC-1698) show non-α7 agonist activity, the tropane-conjugated indole in tropisetron precludes the activation of subtypes other than α7. The sequence alignment of different subunits of the nAChR family suggests that, amongst the loop regions that contribute to the shape of the binding pocket, loop F is a preferred candidate for conferring subtype selectivity to functional regions in the receptors (Supplementary Figure 1). In contrast to loop C, residues in loop F arise from the complementary subunit and show substantial variability in sequence among the nAChRs.

Although anabaseine is a full agonist for both the human and rat α7 receptors, DMXBA and its hydroxy metabolites differ in their efficacy for these two receptors (Kem *et al*, 2004). This discrimination indicates specific interactions of the benzylidene substituents with the receptor. Our structural analysis points to a set of conserved residues in loop F, but not loop C, that determine the relative potency and selectivity of these ligands for the α7 receptor. This is supported by the fact that all BAs produce solvent protection of backbone amide protons in loop F, as shown by hydrogen exchange mass spectrometry (J Shi *et al*, unpublished results). In electrophysiological studies of chimeric and point mutant α7 receptors, residues in loops C, E and F of the receptor

 

LBD that differ across species have been shown to account for the differential pharmacology (Stokes *et al*, 2004). In particular, our structural data point to a Ser substitution of Gly 166 in loop F of human α7 compared with rat α7, which could contribute to a higher efficacy and potency of the 4-OH-DMXBA metabolite for rat versus human α7 receptors, compared with DMXBA. Ser 166, in addition to neighbouring Asp 163 and Ser 165, provides a more favourable polar environment to accommodate the hydroxyl group at 4-position. Similarly, the position and conformation of tropisetron at the binding interface are consistent with an equal efficacy for the human and rat α7 nAChRs (Stokes *et al*, 2004). Conversely, limited modification of a nicotinic ligand, such as the addition of a methyl group to the indole nitrogen of LY278 584, a $5HT_3$ antagonist structurally related to tropisetron (Barnes *et al*, 1992), may generate steric clashes with residues in loop F, consistent with a loss of activity on α7 and α4β2 nAChRs (Macor *et al*, 2001). Hence, loop F represents a major determinant of subtype selectivity among nAChR ligands. Further investigation of other partial agonists with AChBP and how they interact with loop F may provide a more precise understanding of partial agonism in nAChRs.

In summary, our comprehensive structural analysis of AChBP complexes with a non-selective, full nicotinic agonist and three α7-selective partial agonists shows interactions with residue positions in loop F that govern much of the selectivity for these compounds, whereas the closure of loop C is a determinant of agonist efficacy. As the locus of interacting residues within loop F shows high sequence variability within the nAChRs, this region provides a variable surface that should be considered as a template for the design of new subtype-selective drugs with specific pharmacological properties. Further investigation should address the capability of other partial agonists to interact with loop F and induce a variable degree of loop C closure within the binding pocket of nAChRs, and how this might affect the gating process. In addition, we have shown that this family of partial agonists adopts, at least, two orientations within a given pentameric AChBP molecule. This raises the possibility that partial agonism, in at least some cases, might be due to the degree to which active agonist orientations are adopted within a pentameric nAChR. The influence of multiple bound agonist orientations on other α7 receptor properties, such as cooperativity and desensitization (Papke *et al*, 2009), may be relevant in understanding the partial agonism for this and related LGIC receptors.

## Materials and methods

### *Nicotinic ligands*

Anabaseine and its DMXBA and 4-OH-DMXBA derivatives were synthesized as dihydrochloride salts as described by Kem *et al* (2004). Tropisetron hydrochloride and methyllycaconitine citrate were purchased from Tocris (Ellisville, MO). [$^3$H]-epibatidine (SA, 55.5 Ci/mmol) was obtained from Perkin-Elmer (Waltham, MA).

### *Protein expression and purification*

AChBP, flanked by an N-terminal FLAG epitope numbered (−8)DYKDDDDKL(0), was expressed from chemically synthesized cDNA as a soluble exported protein from stably transfected HEK293S cells lacking the *N*-acetylglucosaminyltransferase I (GnTI−) gene and selected for G418 resistance (Hansen *et al*, 2004). Dulbecco's modified Eagle's medium (MediaTech CellGro) containing 2% fetal bovine serum and the secreted AChBP (2–4 mg/l) was collected every 1–3 days for up to 4 weeks, supplemented with 0.02% $NaN_3$ and stored at 4°C. AChBP was purified on immobilized anti-FLAG M2 affinity gel (Sigma) (Hansen *et al*, 2002) by elution using 100 μg/ml FLAG peptide in 50 mM Tris–HCl (pH 7.4), 150 mM NaCl, 0.02% $NaN_3$. Pure AChBP was dialysed against the same buffer and concentrated by ultrafiltration. The assembly, as a stable pentamer, was assessed by analytical size-exclusion chromatography.

### *Radioligand competition assay*

Dissociation constants ($K_d$) for anabaseine, its derivatives and tropisetron were determined by equilibrium competition with [$^3$H]-epibatidine (Talley *et al*, 2006). Briefly, AChBP (500 pM in binding sites), polyvinyltoluene anti-mouse scintillation proximity assay beads (0.1 mg/ml, Amersham Biosciences), monoclonal anti-FLAG M2 antibody from mouse, and [$^3$H]-epibatidine (20 nM for A-AChBP, 5 nM for L-AChBP) were combined with increasing concentrations of the competing ligand in 0.1 M $NaPO_4$ buffer, pH 7.0 (200 μl total volume). Total and non-specific binding were, respectively, determined in the absence and presence of a saturating concentration (15 μM) of the nicotinic antagonist, MLA. The mixtures were allowed to equilibrate at room temperature for at least 2 h before analysis on a LS 6500 liquid scintillation counter (Beckman Scientific). After background subtraction, data were fitted to a sigmoidal dose–response curve (variable slope) and $K_d$ values were calculated from the observed EC50 value (Cheng and Prusoff, 1973) using GraphPad Prism version 4 (San Diego, CA). The reported $K_d$ values (Table II) are represented as means ± s.d. from at least three independent experiments performed in duplicate.

### *Crystallization and data collection*

Complexes were formed with A-AChBP 6.5 mg/ml (260 μM in binding sites; anabaseine complex) or 10.0–12.5 mg/ml (400–500 μM; other three complexes), a 1.5–3-fold molar excess of ligand and, at least, 1 h incubation at room temperature. The crystallization was achieved by vapour diffusion at 18–20°C using a protein-to-well solution ratio of 1:1 (v/v) in 1–2 μl hanging drops. The well solutions were: for the anabaseine complex: 15% PEG-4000, 0.1 M HEPES (pH 7.5), 0.2 M $MgCl_2$; for the DMXBA complex, 13% PEG-4000, 0.1 M HEPES (pH 7.5), 15% isopropanol, 15% glycerol; for the 4-OH-DMXBA complex, 26% PEG-400, 0.1 M HEPES, (pH 7.5), 0.2 M $MgCl_2$; and for the tropisetron complex, 22% PEG-4000, 0.1 M Tris–HCl (pH 7.5), 0.2 M $Li_2SO_4$. Previous attempts to crystallize an anabaseine complex yielded high-resolution structures, but low binding site occupancy by the ligand. To compensate for the low affinity of anabaseine for A-AChBP (cf. Table II), crystals of the anabaseine complex were further soaked into 20 μl of the well solution supplemented with 0.1 mM of freshly dissolved anabaseine and 20% glycerol (24 h, 18°C). Crystals were flash-cooled in liquid nitrogen, directly (anabaseine, DMXBA, 4-OH-DMXBA complexes) or after a rapid soak in the well solution supplemented with 5% glycerol (tropisetron complex). Data were processed using HKL2000 (Otwinowski and Minor, 1997) or Mosflm (Leslie, 1992). All further computing was carried out with the CCP4 program suite (CCP4, 1994) unless otherwise stated.

### *Structure determination and refinement*

The structures of the four complexes were solved by molecular replacement with AMoRe (Navaza, 1994), using the apo A-AChBP pentamer structure (accession code 2BYN) as a search model. For each complex, the initial model was improved by manual adjustment using Xtalview v4.1 (McRee, 1999) or Coot (Emsley and Cowtan, 2004). The initial models were then refined with REFMAC using the maximum likelihood approach (Murshudov *et al*, 1997), incorporating bulk solvent corrections, anisotropic Fo versus Fc scaling and TLS refinement, with each subunit defining a TLS group. Random sets of reflections were set aside for cross-validation purposes. Automated solvent building was carried out using ARP/wARP (Perrakis *et al*, 1999) or Coot (Emsley and Cowtan, 2004). Data collection and refinement statistics are reported in Table I.

The final structures comprise residues His 1–Arg 207/208 for each of the five subunits in the pentamer. The C-terminal dipeptide, Ala 209–Gly 210, could be resolved only for two subunits in the tropisetron complex. High temperature factors and weak electron densities are associated with residues Asn 15–Met 19 (devoid of Pro 18–Met 19 dipeptide in the anabaseine and 4-OH-DMXBA complexes) and residues Tyr 188–Cys 191 at the tip of loop C in

one subunit (4-OH-DMXBA complex). In all structures, most of the N-terminal FLAG epitope and a well-ordered GlcNAc moiety linked to Asn 74 are visible. Apart from flexible loop regions, the residue positions in the five subunits within a pentamer and between pentamers are very similar in the four structures. Bound anabaseine could be fully resolved as a cyclic form in two of the five binding sites per pentamer (labelled A and B in Figure 2A) and as an open-chain ammonium ketone form in two other binding sites (labelled C). A PEG molecule, arising from the crystallization liquor, was observed in the fifth binding site. Limited binding site occupancy by anabaseine might arise from the depletion of the high affinity, cyclic form, resulting from conversion (Zoltewicz *et al*, 1989) to the very low affinity, open-chain ammonium ketone at the pH of crystallization (see Figure 6). In the other three complexes, all five binding sites were fully occupied, consistent with the higher affinity and chemical stability of these compounds compared with anabaseine. The stereochemistry of each structure was analysed using MolProbity (Davis *et al*, 2007); no residues were found in the disallowed regions of the Ramachandran plot.

Atomic coordinates and structure factors of the A-AChBP complexes with anabaseine, DMXBA, 4-OH-DMXBA and tropisetron have been deposited with the Protein Data Bank (see Table I for accession codes). Figure 1 was generated using ChemDraw (CambridgeSoft, Cambridge), Figures 2–5 using PyMOL (DeLano, 2002) and Figure 6 using GraphPad Prism 4.0 (GraphPad Software, San Diego).

### *Crystal packing analysis*

For all structures, systematic analysis of the crystal packing contacts within 4.2 Å of residues Glu 186–Tyr 195 in loop C was carried out using the NCONT program (CCP4). Overall, the residue pair Gln 186–His187 along with Ser 189 at the base of loop C from one to two subunits within each pentamer establish crystal contacts with a neighbouring pentamer. Regardless of the participation, or a lack thereof, of loop C in crystal contacts between adjacent pentamers, its position remains unchanged, indicating that these contacts have no influence on the position of the loop C tip. Instead, residues within the base of loop C may contribute to the large number of crystal packing geometries documented as seen in the large diversity (>20) of space groups and cell dimensions that have been currently reported for crystals of AChBP.

### *Structural comparisons*

Comparisons with other AChBP structures include those of A-AChBP and its epibatidine and MLA complexes (2BYN, 2BYS and 2BYR, Hansen *et al*, 2005), and those of the nicotine-L-AChBP complex (1UW6, Celie *et al*, 2004). The average r.m.s.d. between anabaseine-bound and DMXBA-bound AChBP subunits is 0.45 Å for 211 Cα atoms with deviation up to 1.55 Å for residue Ser 189; between DMXBA-bound and 4-OH-DMXBA-bound AChBP, the deviation is 0.3 Å for 214 Cα atoms; and between DMXBA-bound and tropisetron-bound AChBP, it is 0.36 Å for 213 Cα atoms. The deviation between anabaseine-bound and nicotine-bound AChBP is 1.33 Å for 177 Cα atoms with deviation up to 7 Å for residue Cys190; between anabaseine-bound and epibatidine-bound AChBP, it is 0.53 Å for 211 Cα atoms with largest deviation up to 0.9 Å for the residue Glu 193. The deviation between tropisetron-bound and nicotine-bound AChBP is 1.31 Å for 185 Cα atoms with deviation up to 3 Å for the residue Cys 190; between tropisetron-bound and epibatidine-bound AChBP, it is 0.52 Å for 213 Cα atoms with largest deviation up to 3 Å for the residue Cys 190.

### *Supplementary data*

Supplementary data are available at *The EMBO Journal* Online (http://www.embojournal.org).

## Acknowledgements

We thank Wen-Ru Yu and Kwok-Yiu Ho (UCSD) for assistance in protein expression and purification and in binding assays, respectively; the beamline staff at the ESRF (Grenoble, France) and Cory Ralston at ALS (Berkeley, CA) for assistance in data collection; and Scott Hansen for helpful discussion. This study was supported by USPHS grant R37-GM18360 and UO1-DA019372 (to PT), the Pharmaceutical Research and Manufacturers Association Foundation and USPHS grant T32-GM07752 (to REH and JS); NIH grant MH-061412 (to WRK); a European Commission funding through the SPINE2–COMPLEXES project LSHG–CT–2006–031220 (to YB, PM, GS and SC); a CNRS DREI-SDV travel grant (to PM); and the CNRS for REH visit in Marseille (to YB and PM).

## Conflict of interest

The authors declare that they have no conflict of interest.

## References

Barnes JM, Barnes NM, Costall B, Jagger SM, Naylor RJ, Robertson DW, Roe SY (1992) Agonist interactions with 5-HT3 receptor recognition sites in the rat entorhinal cortex labelled by structurally diverse radioligands. *Br J Pharmacol* **105:** 500–504

Bocquet N, Prado de Carvalho L, Cartaud J, Neyton J, Le Poupon C, Taly A, Grutter T, Changeux JP, Corringer PJ (2007) A prokaryotic proton-gated ion channel from the nicotinic acetylcholine receptor family. *Nature* **445:** 116–119

Bocquet N, Nury H, Baaden M, Le Poupon C, Changeux JP, Delarue M, Corringer PJ (2009) X-ray structure of a pentameric ligand-gated ion channel in an apparently open conformation. *Nature* **457:** 111–114

Bourne Y, Talley TT, Hansen SB, Taylor P, Marchot P (2005) Crystal structure of a Cbtx-AChBP complex reveals essential interactions between snake alpha-neurotoxins and nicotinic receptors. *EMBO J* **24:** 1512–1522

Bouzat C, Gumilar F, Spitzmaul G, Wang HL, Rayes D, Hansen SB, Taylor P, Sine SM (2004) Coupling of agonist binding to channel gating in an ACh-binding protein linked to an ion channel. *Nature* **430:** 896–900

Brejc K, van Dijk WJ, Klaassen RV, Schuurmans M, van Der Oost J, Smit AB, Sixma TK (2001) Crystal structure of an ACh-binding protein reveals the ligand-binding domain of nicotinic receptors. *Nature* **411:** 269–276

Briggs CA, McKenna DG, Piattoni-Kaplan M (1995) Human alpha 7 nicotinic acetylcholine receptor responses to novel ligands. *Neuropharmacology* **34:** 583–590

CCP4 (1994) The CCP4 suite: programs for protein crystallography. *Acta Crystallogr D Biol Crystallogr* **50:** 760–763

Celie PH, van Rossum-Fikkert SE, van Dijk WJ, Brejc K, Smit AB, Sixma TK (2004) Nicotine and carbamylcholine binding to nicotinic acetylcholine receptors as studied in AChBP crystal structures. *Neuron* **41:** 907–914

Changeux JP, Edelstein SJ (2005) Allosteric mechanisms of signal transduction. *Science* **308:** 1424–1428

Cheng Y, Prusoff WH (1973) Relationship between the inhibition constant (K1) and the concentration of inhibitor which causes 50 per cent inhibition (I50) of an enzymatic reaction. *Biochem Pharmacol* **22:** 3099–3108

Davis IW, Leaver-Fay A, Chen VB, Block JN, Kapral GJ, Wang X, Murray LW, Arendall WB, Snoeyink J, Richardson JS, Richardson DC (2007) MolProbity: all-atom contacts and structure validation for proteins and nucleic acids. *Nucleic Acids Res* **35:** W375–W383

de Fiebre CM, Meyer EM, Henry JC, Muraskin SI, Kem WR, Papke RL (1995) Characterization of a series of anabaseine-derived compounds reveals that the 3-(4)-dimethylaminocinnamylidine derivative is a selective agonist at neuronal nicotinic alpha 7/125I-alpha-bungarotoxin receptor subtypes. *Mol Pharmacol* **47:** 164–171

DeLano WL (2002) *The PyMOL Molecular Graphics System*. San Carlos, CA, USA: Delano Scientific, http://www.pymol.org

Dellisanti CD, Yao Y, Stroud JC, Wang ZZ, Chen L (2007) Crystal structure of the extracellular domain of nAChR alpha1 bound to alpha-bungarotoxin at 1.94 Å resolution. *Nat Neurosci* **10:** 953–962

 

Emsley P, Cowtan K (2004) Coot: model-building tools for molecular graphics. *Acta Crystallogr D Biol Crystallogr* **60:** 2126–2132

Freedman R, Olincy A, Buchanan RW, Harris JG, Gold JM, Johnson L, Allensworth D, Guzman-Bonilla A, Clement B, Ball MP, Kutnick J, Pender V, Martin LF, Stevens KE, Wagner BD, Zerbe GO, Soti F, Kem WR (2008) Initial phase 2 trial of a nicotinic agonist in schizophrenia. *Am J Psychiatry* **165:** 1040–1047

Gao F, Bern N, Little A, Wang HL, Hansen SB, Talley TT, Taylor P, Sine SM (2003) Curariform antagonists bind in different orientations to acetylcholine-binding protein. *J Biol Chem* **278:** 23020–23026

Hansen SB, Radic Z, Talley TT, Molles BE, Deerinck T, Tsigelny I, Taylor P (2002) Tryptophan fluorescence reveals conformational changes in the acetylcholine binding protein. *J Biol Chem* **277:** 41299–41302

Hansen SB, Sulzenbacher G, Huxford T, Marchot P, Taylor P, Bourne Y (2005) Structures of *Aplysia* AChBP complexes with nicotinic agonists and antagonists reveal distinctive binding interfaces and conformations. *EMBO J* **24:** 3635–3646

Hansen SB, Talley TT, Radic Z, Taylor P (2004) Structural and ligand recognition characteristics of an acetylcholine-binding protein from *Aplysia californica*. *J Biol Chem* **279:** 24197–24202

Hilf RJ, Dutzler R (2008) X-ray structure of a prokaryotic pentameric ligand-gated ion channel. *Nature* **452:** 375–379

Hilf RJ, Dutzler R (2009) Structure of a potentially open state of a proton-activated pentameric ligand-gated ion channel. *Nature* **457:** 115–118

Ho KY, Gan TJ (2006) Pharmacology, pharmacogenetics, and clinical efficacy of 5-hydroxytryptamine type 3 receptor antagonists for postoperative nausea and vomiting. *Curr Opin Anaesthesiol* **19:** 606–611

Hogg RC, Bertrand D (2007) Partial agonists as therapeutic agents at neuronal nicotinic acetylcholine receptors. *Biochem Pharmacol* **73:** 459–468

Hoyer D, Boddeke HW (1993) Partial agonists, full agonists, antagonists: dilemmas of definition. *Trends Pharmacol Sci* **14:** 270–275

Karlin A (2002) Emerging structure of the nicotinic acetylcholine receptors. *Nat Rev Neurosci* **3:** 102–114

Kem WR (2000) The brain alpha7 nicotinic receptor may be an important therapeutic target for the treatment of Alzheimer's disease: studies with DMXBA (GTS-21). *Behav Brain Res* **113:** 169–181

Kem WR, Mahnir VM, Papke RL, Lingle CJ (1997) Anabaseine is a potent agonist on muscle and neuronal alpha-bungarotoxin-sensitive nicotinic receptors. *J Pharmacol Exp Ther* **283:** 979–992

Kem WR, Mahnir VM, Prokai L, Papke RL, Cao X, LeFrancois S, Wildeboer K, Prokai-Tatrai K, Porter-Papke J, Soti F (2004) Hydroxy metabolites of the Alzheimer's drug candidate 3-[(2,4-dimethoxy)benzylidene]-anabaseine dihydrochloride (GTS-21): their molecular properties, interactions with brain nicotinic receptors, and brain penetration. *Mol Pharmacol* **65:** 56–67

Kem W, Soti F, Wildeboer K, LeFrancois S, MacDougall K, Wei D-Q, Chou K-C, Arias H (2006a) The nemertine toxin anabaseine and its derivative DMXBA (GTS-21): chemical and pharmacological properties. *Mar Drugs* **4:** 255–273

Kem WR, Wildeboer KM, MacDougall KN, Soti F (2006b) The active form of the nicotinic receptor agonist anabaseine is the cyclic iminium cation. *Soc Neurosci Mtg Abstr* **722:** 12

Lape R, Colquhoun D, Sivilotti LG (2008) On the nature of partial agonism in the nicotinic receptor superfamily. *Nature* **454:** 722–727

Leslie AG (1992) Recent changes to the MOSFLM package for processing film and image plate data. *Joint CCP4–ESF-EAMCB Newsl Protein Crystallogr* **26**

Machu TK, Hamilton ME, Frye TF, Shanklin CL, Harris MC, Sun H, Tenner TE, Soti FS, Kem WR (2001) Benzylidene analogs of anabaseine display partial agonist and antagonist properties at the mouse 5-hydroxytryptamine(3A) receptor. *J Pharmacol Exp Ther* **299:** 1112–1119

Macor JE, Gurley D, Lanthorn T, Loch J, Mack RA, Mullen G, Tran O, Wright N, Gordon JC (2001) The 5-HT3 antagonist tropisetron (ICS 205–930) is a potent and selective alpha7 nicotinic receptor partial agonist. *Bioorg Med Chem Lett* **11:** 319–321

Malany S, Osaka H, Sine SM, Taylor P (2000) Orientation of alpha-neurotoxin at the subunit interfaces of the nicotinic acetylcholine receptor. *Biochemistry* **39:** 15388–15398

Martin EJ, Panikar KS, King MADeyrup M, Hunter B, Wang G, Meyer EM (1994) Cytoprotective actions of 2,4-dimethoxybenzylidene anabaseine in differentiated PC12 cells and septal cholinergic cells. *Drug Dev Res* **31:** 134–141

McRee DE (1999) XtalView/Xfit—a versatile program for manipulating atomic coordinates and electron density. *J Struct Biol* **125:** 156–165

Murshudov GN, Vagin AA, Dodson EJ (1997) Refinement of macromolecular structures by the maximum-likelihood method. *Acta Crystallogr D Biol Crystallogr* **53:** 240–255

Navaza J (1994) AMoRe: an automated package for molecular replacement. *Acta Crystallogr Sect A* **50:** 157–163

Olincy A, Harris JG, Johnson LL, Pender V, Kongs S, Allensworth D, Ellis J, Zerbe GO, Leonard S, Stevens KE, Stevens JO, Martin L, Adler LE, Soti F, Kem WR, Freedman R (2006) Proof-of-concept trial of an alpha7 nicotinic agonist in schizophrenia. *Arch Gen Psychiatry* **63:** 630–638

Otwinowski Z, Minor W (1997) Processing of X-ray diffraction data collected in oscillation mode. *Methods Enzymol* **276:** 307–326

Papke RL, Kem WR, Soti F, Lopez-Hernandez GY, Horenstein NA (2009) Activation and desensitization of nicotinic α7-type acetylcholine receptors by benzylidene anabaseines and nicotine. *J Pharmacol Exp Ther* **329:** 791–807

Papke RL, Meyer EM, Lavieri S, Bollampally SR, Papke TA, Horenstein NA, Itoh Y, Porter Papke JK (2004) Effects at a distance in alpha 7 nAChR selective agonists: benzylidene substitutions that regulate potency and efficacy. *Neuropharmacology* **46:** 1023–1038

Papke RL, Schiff HC, Jack BA, Horenstein NA (2005) Molecular dissection of tropisetron, an alpha7 nicotinic acetylcholine receptor-selective partial agonist. *Neurosci Lett* **378:** 140–144

Perrakis A, Morris R, Lamzin VS (1999) Automated protein model building combined with iterative structure refinement. *Nat Struct Biol* **6:** 458–463

Pratt WB, Taylor P (1990) In *Principles of Drug Action. The Basis of Pharmacology*, Pratt WB, Taylor P (eds). New York: Churchill Livingstone

DeLano WL (2008) *The PyMOL Molecular Graphics System*. Palo Alto, CA, USA: DeLano Scientific LLC

Shi J, Koeppe JR, Komives EA, Taylor P (2006) Ligand-induced conformational changes in the acetylcholine-binding protein analyzed by hydrogen-deuterium exchange mass spectrometry. *J Biol Chem* **281:** 12170–12177

Shimohama S, Greenwald DL, Shafron DH, Akaika A, Maeda T, Kaneko S, Kimura J, Simpkins CE, Day AL, Meyer EM (1998) Nicotinic alpha 7 receptors protect against glutamate neurotoxicity and neuronal ischemic damage. *Brain Res* **779:** 359–363

Stephenson RP (1956) A modification of receptor theory. *Br J Pharmacol Chemother* **11:** 379–393

Stokes C, Papke JK, Horenstein NA, Kem WR, McCormack TJ, Papke RL (2004) The structural basis for GTS-21 selectivity between human and rat nicotinic alpha7 receptors. *Mol Pharmacol* **66:** 14–24

Talley TT, Harel M, Hibbs RE, Radic Z, Tomizawa M, Casida JE, Taylor P (2008) Atomic interactions of neonicotinoid agonists with AChBP: molecular recognition of the distinctive electronegative pharmacophore. *Proc Natl Acad Sci USA* **105:** 7606–7611

Talley TT, Yalda S, Ho KY, Tor Y, Soti FS, Kem WR, Taylor P (2006) Spectroscopic analysis of benzylidene anabaseine complexes with acetylcholine binding proteins as models for ligand-nicotinic receptor interactions. *Biochemistry* **45:** 8894–8902

Taylor P (2006) Agents acting at the neuromuscular junction and autonomic ganglia. In *Goodman and Gilman's The Pharmacological Basis of Therapeutics*, Brunton LL, Lazo JS, Parker KL (eds) pp 217–236. New York: McGraw-Hill

Unwin N (2005) Refined structure of the nicotinic acetylcholine receptor at 4A resolution. *J Mol Biol* **346:** 967–989

Zhang R, White NA, Soti FS, Kem WR, Machu TK (2006) N-terminal domains in mouse and human 5-hydroxytryptamine3A receptors confer partial agonist and antagonist properties to benzylidene analogs of anabaseine. *J Pharmacol Exp Ther* **317:** 1276–1284

Zoltewicz JA, Bloom LB, Kem WM (1989) Quantitative determination of the ring-chain hydrolysis equilibrium constant for anabaseine and related tobacco alkaloids. *J Org Chem* **54:** 4462–4468